JCI The Journal of Clinical Investigation

Immune synapses between mast cells and γδ T cells limit viral infection

Chinmay Kumar Mantri, Ashley L. St. John

J Clin Invest. 2018. https://doi.org/10.1172/JCI122530.

Research In-Press Preview Immunology Infectious disease

Graphical abstract

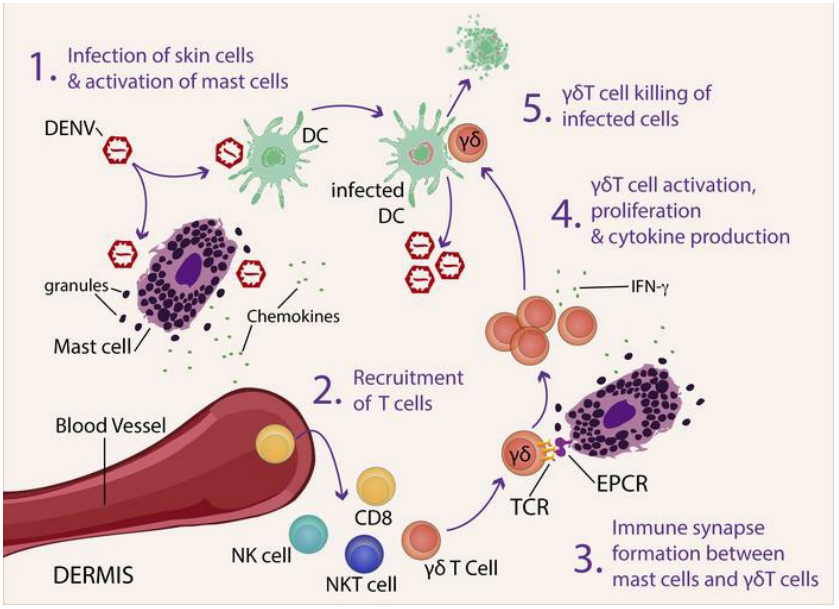

Find the latest version:

https://jci.me/122530/pdf

Immune synapses between mast cells and γδ T cells limit viral infection

Chinmay Kumar Mantri[1], Ashley L. St. John[1,2,3]*

[1]Program in Emerging Infectious Diseases, Duke-National University of Singapore Medical School, 169857, Singapore.

[2]Department of Pathology, Duke University Medical Center, Durham, North Carolina, 27705, USA

[3]Department of Microbiology and Immunology, Young Loo Lin School of Medicine, National University of Singapore, Singapore

Conflict of interest declaration: The authors have declared that no conflict of interest exists.

*Correspondence may be addressed to:

Ashley St. John, Ph.D.
Program in Emerging Infectious Diseases
Duke-National University of Singapore Medical School
8 College Rd., Level 9
169857, Singapore
Tel: +65 9771-7231
Email: ashley.st.john@duke-nus.edu.sg

ABSTRACT

Mast cells (MCs) are immune sentinels but whether they also function as antigen-presenting cells (APCs) remains elusive. Using mouse models of MC-deficiency, we report MC-dependent recruitment and activation of multiple T cell subsets to the skin and draining lymph nodes (LNs) during dengue virus (DENV) infection. Newly-recruited and locally-proliferating γδT cells were the first responding T cell subset to MC-driven inflammation and their production of IFN-γ was MC-dependent. MC-γδ T cell conjugates were observed consistently in infected peripheral tissues, suggesting a new role for MCs as non-conventional APCs for γδT cells. MC-dependent γδT cell activation and proliferation during DENV infection required TCR signaling and the non-conventional antigen presentation molecule EPCR on MCs. γδT cells, not previously implicated in DENV host defense, killed infected target dendritic cells and contributed to clearance of DENV in vivo. We believe immune synapse formation between MCs and γδT cells is a novel mechanism to induce specific and protective immunity at sites of viral infection.

INTRODUCTION

MCs are tissue resident cells that are distributed throughout the dermis, where they have an evolutionarily conserved responsibility to the host for pathogen surveillance (1). Although they have been long-associated with pathological conditions including asthma and allergy (2), they are also now well accepted to be sentinel cells that send an alarm to the immune system that a pathogen is present. MCs perform this task efficiently and recognize multiple classes of pathogens by detecting bacterial or viral structural components using a wide range of traditional pathogen associated molecular patterns (e.g. TLRs) (3). MCs are also activated by indirect, endogenous signals of infection (such as to complement) (1). When activated, MCs respond with a biphasic response, within seconds releasing pre-formed mediators that are packed tightly into granules while initiating pro-inflammatory transcriptional programs. The second phase of the response involves releasing these de novo-produced cytokines and chemokines in the hours following activation (1). MC innate responses to pathogens promote pathogen clearance in vivo through initiating inflammation and recruitment and activation of other immune cells within the site of infection. Although MCs are well established to play a role in host defense against bacteria and parasites, MC responses to viral pathogens had hardly been examined until recently (1, 4). MCs degranulate strongly to dengue virus (DENV), a clinically relevant

Flavivirus that infects the skin after mosquito bite. DENV activation of MCs promotes immune clearance of DENV in the skin and in draining lymph nodes (LNs), which is characterized by recruitment of cytotoxic lymphocytes, such as NK cells and NKT cells to DENV infection sites by MCs (5). This raises a question of whether other subtypes of lymphocytes are recruited to the peripheral sites of infection by MCs and what impact this interaction could have functionally on viral clearance.

There is increasing evidence for MC interaction with T cells in tissues. For example, in addition to NKT cell recruitment during DENV infection, it has been shown that MCs promote the recruitment of $CD8^+$ T cells during Newcastle virus infection (6). MCs responding to viral pathogens have been shown to produce several chemokines that are understood to promote the recruitment of various subsets of T cells, including CCL5, CXCL10, CXCL12, CX3CL1 (5-7). In addition to directing chemotaxis, MCs also prompt endothelial activation, which is required for extravasation from the blood vessel lumen into tissues (8). An important component of this is MC-derived TNF, which induces E-selectin expression on vascular endothelium (9). Aside from cellular recruitment, MCs could potentially influence T cell responses through other mechanisms. For example, MC-derived pre-formed TNF is required for the LN hypertrophy (retention of B and T cells in LNs) that occurs in the hours after acute inflammation is initiated (10). This response is thought to be essential for optimal immune specificity since it increases the probability that rare antigen-specific T cells are present in draining LNs as the adaptive immune response is undergoing refinement.

Due to discordant results from in vitro and in vivo studies (11), the question of whether MCs are physiologically relevant as APCs remains unanswered. Our understanding is further obstructed by the fact that MCs provoke antigen-independent activation of T cells in co-culture experiments (12, 13), so whether antigen presentation in a traditional sense occurs has remained unclear. MCs do not constitutively express MHC-II molecules on their surface in the skin, although MHC-II is inducible on MCs in various inflammatory and experimental contexts

(14). MCs also express some non-classical MHC molecules, such as CD1d (15). In spite of the divergent data regarding whether MCs can serve as APCs in vivo, there is consensus that MCs have been described to physically interact with T cells in tissue sections (16) with the function and mechanisms of this interaction unknown.

Aside from MCs, there are other immune cells that reside in peripheral tissues and contribute to innate immune responses. For example, γδ T cells patrol the skin, although not much is known about their function in immune responses and the mechanisms that lead to their activation (17, 18). However, γδ T cells have been implicated in the clearance of West Nile virus infection (19, 20), which is closely related to DENV and also injected into the skin by mosquitos. Typically, γδ T cells are not restricted to recognition of antigen bound to MHC molecules (17) and they have the ability to become activated by certain stimuli completely independent of antigen presentation (21), suggesting that they may not need signals from other cells or contact with them to become activated. Both γδ T cells and MCs inhabit the same peripheral milieu, both cell types serve a bridging function between innate and adaptive immunity and are responsible for host defense and pathogen clearance. However, interactions between MCs and γδ T cells have not been reported or postulated.

In this study, we sought to understand the contributions of MCs to the trafficking and activation of various T cells subsets in the skin during acute viral infection. Our data show that not only are MCs consequential to the regulated trafficking of multiple subsets of T cells during viral infection, they contribute significantly to the early recruitment, activation and proliferation of γδ T cells, through the non-conventional antigen presentation molecule EPCR, in a γδ TCR-signaling dependent manner involving immune synapse formation. In turn, γδ T cells enhance clearance of virus in vivo, emphasizing the functional significance of the physical interaction between MCs and γδ T cells.

RESULTS

Mast cells recruit multiple subsets of T cells to virus infection sites. To investigate the role of MCs in potentiating T cell responses during cutaneous viral infection, we injected 1×10^5 pfu of DENV2 subcutaneously into the mouse footpad (FP) skin of MC-sufficient C57Bl/6 mice and congenic MC-deficient *Kit* $^{W\text{-}sh/W\text{-}sh}$ "Sash" mice, which have an inversion in the c-*kit* promoter that impedes development of the MC lineage (22). We infected mice by peripheral injection to replicate the natural route of infection for DENV in humans. The skin of the FPs was removed and processed to single cell suspensions and stained for flow cytometry using a panel of antibodies designed to identify various subsets of T cells at the site of infection (**Figure S1**). Previously, we showed that DENV induces strong MC degranulation in vivo, with approximately 30% of MCs losing granularity in the skin following infection and recruitment of NK and NKT cells into the skin (5), but the responses of additional T cell subsets were not evaluated. Here, when FPs were infected with DENV, we observed that multiple subsets of T cells were enriched in the skin in a MC-dependent manner (**Figure 1A-E**). The subsets of T cells dominating the early cutaneous response were innate T cells, including NKT cells (**Figure 1B**) and γδ T cells (**Figure 1C**). $CD8^+$ T cells also showed MC-dependent enrichment but at a later time point of day 3 post-infection (**Figure 1D**), while $CD4^+$ T cells were not enriched significantly in the skin of MC-sufficient mice over MC-deficient, Sash mice until day 5 post-infection (**Figure 1E**). Reconstitution of Sash mice with bone marrow-derived MCs (BMMCs), Sash-R resulted in restored recruitment of total T cells and the numbers of NKT and γδ, CD4 and CD8 T cell subsets in the skin were also restored to the levels of DENV-infected WT mice (**Figure S2A-E**), confirming the MC-dependency of various subsets of T cells during DENV. Furthermore, when we measured the activation status of the recruited T cells, we found that day 3 was a critical time point for T cell activation in the FP following DENV infection. In Sash mice lacking MCs, there was substantially reduced activation of $CD8^+$, NKT and γδ T cells at the site of infection

compared to WT and reconstituted Sash mice, Sash-R (**Figure 1F-H**). In contrast, activation of $CD4^+$ T cells was not influenced by MCs (**Figure 1I**). Importantly, these defects in T cell recruitment were observed in the skin of Sash mice compared to WT and Sash-R mice, even though viral titers were higher in Sash mice than either WT or Sash-R mice suggesting that this deficit was not due to the lower viral burden in Sash mice (**Figure 1J, S2F**). Together these data demonstrate that T cell recruitment and activation at the site of cutaneous DENV infection is MC-dependent and occurred in response to stimuli from MCs.

Mast cells induce retention and activation of T cells in the draining lymph node. The arrival of activated DCs and sequestration of T cells from the circulation that occur during LN hypertrophy provide an optimal environment for the initiation of adaptive immune responses by increasing the likelihood of T cell encounter with their DC-presented cognate antigens (23). Since DENV has been shown to induce a strong degranulation response in MCs and since particulate TNF released by MCs is a potent inducer of LN hypertrophy, we investigated which subsets of T cells were retained in the popliteal LN, which is the draining LN for the FP skin (**Figure 2**). Although we observed retention of multiple subsets of T cells in the draining LNs of DENV-infected Sash mice, the magnitude of the total T cell response was significantly lower in comparison to the WT mice, indicating that a significant portion of this response is due to the involvement of MCs in immunosurveillance for DENV (**Figure 2A**). T cell subsets with innate functions, including NKT cells and γδ T cells, were recruited to draining LNs in enhanced numbers in WT mice compared to Sash (**Figure 2B,C**), and showed significantly increased levels of activation (**Figure 2D,E**) at multiple time points post-infection. We also observed a MC-dependent increase in the total numbers and activation of $CD8^+$ T cells at 24h and 48h post-infection in WT mice compared to Sash mice (**Figure 2F,G**), which is consistent with LN hypertrophy and initiation of adaptive responses against DENV. Moreover, the total numbers of $CD8^+$ T cells were significantly higher in WT mice compared to Sash mice at various time points

post-infection (**Figure 2F**). Similarly, $CD4^+$ T cell numbers were augmented throughout the time course, assayed in WT mice compared to Sash mice, but numbers of activated $CD4^+$ T cells were only significantly increased in WT mice 24h post-infection (**Figure 2H,I**). Interestingly, the peak γδ T cell activation occurred at 3d post-infection (**Figure 2E**), similar to the FP skin (**Figure 1G**). Experiments using Sash-R mice further confirmed that MCs were sufficient to restore the phenotype of enhanced T cell recruitment and activation that was diminished due to MC-deficiency (**Figure S3**). With regards to the innate T cells that we assessed, we noted that γδ T cells were more abundant in the draining LN during DENV infection and activation peaked earlier than NKT cells, indicating that γδ T cells are the likely the first innate T cells to respond to DENV infection.

Validation of MC-dependent T cell recruitment with Mcpt5-cre/iDTR mice. To further validate our results of MC-dependent T cell recruitment and activation during DENV infection and rule out any effect that the *c-kit* mutation might have on the function of other hematopoietic cells, we employed a second mouse model that is used to assess MC function, the *Mcpt5*-cre/iDTR MC ablation model (24). For this, mice with cre driven by the MC-specific promoter of *Mcpt5* were crossed with mice bearing an inducible diphtheria toxin receptor (iDTR) to produce mice (*Mcpt5*-cre/iDTR) that express the diphtheria toxin receptor only on MCs (24). These mice were injected with diphtheria toxin (DT) at regular intervals using a protocol developed by others (24) to strongly reduce the numbers of peripheral MCs before infecting them with DENV2 (**Figure 3A**). MC depletion was validated to be >95% (**Figure S4**). Consistent with our data from Sash mice (**Figures 1, 2**), in this alternate model of MC-deficiency, we observed impaired total T cell retention in the draining LN of MC-depleted *Mcpt5*-cre/iDTR mice compared to DT-injected *Mcpt5*-cre congenic controls (**Figure 3B**). This reduction in T cell retention was consistent for multiple subsets of T cells including NKT, γδ T cells, $CD8^+$ and $CD4^+$ T cells (**Figure 3C-F**). Thus, these results using a *c-kit*-independent MC-selective ablation model,

validate our finding that MCs recruit multiple subsets of T cells, including γδ T cells, to the draining LN.

MC-dependent γδ T cell recruitment, proliferation and activation during infection. Since γδ T cells were the first T cells to respond at the site of infection (**Figure 1C**) and draining LN (**Figure 2C**), we next aimed to determine if the increase in the numbers of γδ T cells at virus-infected sites was due to proliferation in response to infection or recruitment directly from the circulation. To distinguish between these two populations and assess the contributions of MCs to each, we labeled local FP-resident cells by injecting CFSE into the FPs prior to infection with DENV in WT and Sash mice. At the concentration of CFSE used, within 4h, CFSE had labeled ~50% of the FP-resident DCs, while <1% of the LN cells were labeled (**Figure S5**), indicating that the presence of $CFSE^+$ cells in LNs following DENV challenge can be interpreted as showing they are FP-derived. Our results also suggested that local FP-resident γδ T cells underwent proliferation *in situ*, as evident by the increase in the total numbers of $CFSE^+$ γδ T cells in the FP during infection (**Figure 4A**). In addition to the significant increase in total γδ T cells (**Figure 4A**), there was a population of newly-recruited or possibly unlabeled proliferating γδ T cells in the FP in response to infection that were CFSE-negative at 24h post-infection (**Figure 4A**). In MC-deficient Sash mice, both $CFSE^+$ (FP resident) and $CFSE^-$ populations were significantly reduced during infection compared to WT mice (**Figure 4A**). There was no baseline difference in the levels of resident or unlabeled γδ T cells between WT and Sash mice in un-infected control groups (**Figure 4A**). We also observed numbers of $CFSE^-$ γδ T cells were increased in draining LNs following infection of WT mice with DENV (**Figure 4B**). Similar statistically significant trends in MC-dependent γδ T cell recruitment in response to DENV in FPs and draining LNs persisted at 72h post-infection (**Figure S6**). Of note, the FP-derived γδ T cells in the draining LN displayed evidence of having proliferated based on dilution of the CFSE stain (**Figure 4C-D, S7**).

Increased numbers of $CFSE^-$ γδ T cells suggestive of recruitment to the LN; however, due to the possibility that the increase in unlabeled γδ T cells could also occur if there were to be substantial proliferation of the unlabeled local cells, we also confirmed that recruitment occurs using an alternative method. For this, labeled splenocytes were injected into mice prior to DENV infection, and we measured the $CFSE^+$ T cells and that trafficked from the circulation into the FP skin (**Figure 4E**) and LN (**Figure 4F**) by 24h post-infection. This confirmed that recruitment occurs, in addition to local proliferation, in a MC-dependent fashion. Similarly, MC-dependent recruitment of the γδ T cell subset in response to DENV in FPs and draining LNs was also observed (**Figure S8**). These results establish that the population of γδ T cells that is augmented by MCs during DENV infection consists of both newly recruited and locally proliferating γδ T cells. Both recruitment and proliferation occur significantly and are MC-dependent.

Functional γδ T cell responses rely on induction of IFN-γ in the context of both viral infection and tumor immunosurveillance (18). Thus, to further assess the contributions of MCs to γδ T cell activation in vivo, we quantified the numbers of IFN-γ producing γδ T cells (**Figure 4G**) in comparison to IFN-γ-producing $CD8^+$ (**Figure 4H**) and $CD4^+$ (**Figure 4I**) T cells during DENV infection of WT, Sash and Sash-R mice. Interestingly, IFN-γ production by γδ T cells at both 24h and 48h was highly dependent on MCs (**Figure 4G**). Although $CD8^+$ T cells were not major contributors of IFN-γ, there were also reduced numbers of $CD8^+IFN\text{-}\gamma^+$ T cells at 48h post-infection in Sash mice compared to WT and Sash-R mice (**Figure 4H**); however, MCs did not significantly influence the number of $CD4^+IFN\text{-}\gamma^+$ T cells (**Figure 4I**). These results demonstrate that IFN-γ production by γδ T cells is MC-dependent and indicate that γδ T cells are a major cellular source of IFN-γ during DENV infection.

Contact is necessary for MC-dependent γδ T cell activation and proliferation. Having identified MC-dependent γδ T cell activation and proliferation in virus-infected skin, we next

questioned whether the influence of MCs on γδ T cells was direct and capable of activating γδ T cells in the absence of other bystander cells of the tissue microenvironment. To begin to address this question, we performed a trans-well assay where T cells purified from the LNs of naïve mice were applied to the upper compartment of the semi-porous chamber and BMMCs were added to the bottom chamber, with and without DENV2 as a stimulus (**Figure 5A**). Although MCs are highly resistant to infection by DENV (5), we included additional controls using bone marrow-derived macrophages (BMMΦ) to determine whether virus-infected cells could also induce responses similar to DENV-activated MCs (**Figure 5A**). Consistent with our in vivo experiments, we observed enhanced migration of total T cells to the bottom chamber when BMMCs were exposed to DENV, indicating virus-induced MC activation is directly important for recruitment of T cells (**Figure 5B**). In contrast, there was no enhanced recruitment of T cells by DENV-infected BMMΦs (**Figure 5B**). Furthermore, the γδ T cell population was preferentially enriched amongst the T cell subsets that migrated to the lower chamber towards DENV-activated BMMCs (**Figure 5C**). We observed that the ratio of activated γδ T cells in the lower chamber (contact with MCs) relative to the upper chamber (no contact with MCs) was significantly higher when BMMCs were stimulated with DENV, but not in any other control groups (**Figure 5D**). These data suggest that activation of γδ T cells is both virus-dependent and MC-dependent since it occurred only when γδ T cells came in contact with DENV-exposed MCs. However, in contrast, there was no migration and activation of γδ T cells in response to infected BMMΦs (**Figure 5D**), highlighting a unique capacity of MCs to recruit and activate γδ T cells.

To identify stimuli that might promote recruitment of γδ T cells by MCs, we measured the expression of known γδ T cell chemoattractants by RT-PCR. Our results show that CXCL10 was highly induced in MCs upon stimulation with DENV (**Figure 5E**). We also observed an increase in expression of other chemoattractants that are known to promote T cell migration including CCL2, CCL20, CCL25 and CCL27 (**Figure 5E**). We also selected two of these

chemokines to confirm increased cytokine production occurs at the protein level, CCL2 and CXCL10. By intracellular staining of BMMCs, we observed significant induction of both CCL2 and CXCL10 in DENV-exposed BMMCs (**Figure 5F**). To further characterize the effects of virus-activated MCs on the stimulation and proliferation of γδ T cells, we performed a co-culture experiment where T cells isolated from LNs were incubated with BMMCs in presence or absence of DENV for 96h. Here, MCs promoted relative expansion of γδ T cells (**Figure 5G**) and $CD4^+$ T cells (**Figure 5H**), with no significant influence on the $CD8^+$ T cell population (**Figure 5I**). Although we have noted some degree of γδ T cell activation in the presence of MCs alone, DENV-specific MC-induced γδ T cell activation was significantly higher (**Figure 5G**) and began as early as 48h post infection (**Figure S9**). This basal increase in MC activation is likely due to soluble factors produced by MCs that are able to act on γδ T cells due to their close proximity in the co-culture system. In support of this, we observed that the leukotriene receptor antagonist but not TNF-blocking antibody was able to reduce the basal levels of MC activation in co-culture, although not eliminate it completely (**Figure S10**), suggesting multiple factors may be involved. These results show that specific activation of both αβ and γδ T cells can occur by MCs but, interestingly, γδ T cells showed the highest expansion and percentage activation compared to $CD4^+$ and $CD8^+$ T cells (**Figure 5G-I**). Survival of MCs was not influenced over the course of the experiment (data not shown). To validate the MC- and DENV-dependent expansion of γδ T cells, purified cells from naive mice were labeled with CFSE prior to co-culture with BMMCs and the percentage of γδ T cells undergoing proliferation was measured by flow cytometry (**Figure 5J**). Significantly increased proliferation was apparent when MCs were co-cultured with γδ T cells, compared to controls, and this was further increased in the presence of DENV (**Figure 5J, S11**). CFSE dilution occurred in live cells and appeared step-wise on histograms, confirming the dilution effect was due to proliferation (**Figure S12**). Thus, activation and proliferation of γδ T cells are both MC-dependent and DENV-dependent.

Immune synapse formation between MCs and γδ T cells in vivo

After establishing the potential of DENV-exposed MCs to activate T cells in vitro we questioned whether this occurs in vivo. DENV-infected skin was isolated 24h after subcutaneous injection with virus or saline as a control. This tissue was cryo-sectioned and stained for blood vessels, MCs, and γδ T cells. As MCs are tissue resident and γδ T cells patrol the skin constitutively, we expected to see both cell types in control tissues. Indeed, although γδ T cells were not present in all fields of view (**Figure 6A**), they could be infrequently located but did not show any clear interactions with MCs (**Figure 6B**). In contrast, in DENV-infected skin, MC and γδ T cell interactions were widely observed. In some cases, we identified clusters of γδ T cells that appeared very close to activated MCs (**Figure 6C**). In this case, MC activation was clear due to the presence of extracellular granules near the MCs, suggesting recent degranulation (**Figure 6C**). These γδ T cells could potentially be at high density due to proliferation *in situ* or due to recruitment from the proximal blood vessel, since we observed that both proliferation and recruitment occur in a MC-dependent fashion in the FP during DENV infection (**Figure 4A, E**). Interestingly, we observed physical interactions between γδ T cells and MCs, supported by the presence of multiple γδ T cell – MC conjugates in the same field of view in a representative image (**Figure 6D**). Quantified across multiple fields of view from multiple animals, we determined that approximately 36% of granulated MCs appeared to physically contact γδ T cells at the skin infection site (**Figure S13**). Similarly, 24h after injection of DENV into the peritoneal cavity, conjugates of MCs and γδ T cells could be observed (**Figure 6E**). After cytospinning and staining the peritoneal lavage cells for CD3, γδ TCR, tubulin and MC-heparin, the nature of the physical interactions could be more clearly discerned. Contact sites between γδ T cells and MCs showed strong polarization and clustering of the γδ TCR and signaling molecule CD3 towards the MC (**Figure 6E, S14A**), while γδ T cells were not identified as interacting with MCs in cytospins from control animals (**Figure 6F, S14B**). Additional representative images from DENV infected and control skin and from cytospins of peritoneal

cells after i.p. infection or saline injection, including of multiple γδ T cell – MC conjugates from cells of DENV-infected animals, are provided in **Figure S14**. These images show the extensive recruitment and physical association of MCs and γδ T cells in vivo during DENV infection and, furthermore, suggest antigen presentation by MCs due to the consistent polarization of the γδ TCR during immune synapse formation.

TCR-dependent activation of γδ T cells by MCs

To address the functional consequences of γδ T cells to immune clearance during DENV infection, we examined their ability to kill infected cells. Since DCs are targets of DENV infection in vivo we used DENV-infected bone marrow derived DCs (BMDCs) in co-culture with total T cells to assess target cell killing. There was a significant increase in cytotoxicity in DENV2-infected BMDCs that were exposed to total purified T cells, which was lost after depletion of γδ T cells from the total T cell pool (**Figure 7A**), this indicates that γδ T cells do, indeed, kill DENV-infected DCs. The death of the DENV-infected DCs by γδ T cells was also confirmed by an alternate method, by measuring DC apoptosis by flow cytometry (**Figure S15**). In contrast, BMMCs that were exposed to DENV were not killed (**Figure 7B**), likely due to their resistance to productive DENV infection (5). These results support that γδ T cells are capable of direct killing of infected target cells, but that the interactions between MCs and γδ T cells do not involve target killing.

Based on the appearance of immune synapse formation between MCs and γδ T cells (**Figure 6E**), evidence for γδ T cell activation and proliferation (**Figure 5D,F**) and the confirmation that this interaction does not involve direct killing of MCs (**Figure 7B**), we strongly suspected a process similar to antigen presentation by MCs to γδ T cells was occurring, involving activation of γδ TCR. To determine whether MCs activate γδ T cells through the TCR, we used the specific inhibitor of MEK/ERK-pathway, MEK162, which is required for TCR signaling (25, 26). T cells were cultured with and without MCs and DENV, after which the

activation (**Figure 7C**) and proliferation (**Figure 7D**) of the γδ T cell subset was measured. MCs alone induced activation and proliferation of γδ T cells, which was further increased by DENV (**Figure 7C-D**). Inhibition of TCR signaling blocked the MC- and DENV-dependent activation and proliferation of γδ T cells, but not the MC-dependent and DENV-independent activation (**Figure 7C-D**). This supports that MCs activate γδ T cells and induce their proliferation, which occurs mechanistically through the γδ TCR in the presence of virus.

To identify the mechanism of γδ T cell activation by MCs, we co-cultured MCs with T cells and pulled-down the γδ TCR using a monoclonal antibody. By western blotting, TCRγ was observed in the whole cell lysates from T cell-MC co-cultures (**Figure 7E**). EPCR could also be specifically detected in the lysate fractions (**Figure 7E**). Western blot analysis on the fractions after TCRγδ pull-down confirmed pull-down of the TCRγ subunit and also revealed that Endothelial cell protein C receptor (EPCR) was a protein associated with TCRγδ (**Figure 7F**). Use of an isotype control antibody for pull-down confirmed the specificity of this interaction (**Figure 7F**). EPCR is a trans-membrane glycoprotein and non-conventional antigen presentation molecule closely related to CD1d that has previously been described to interact with γδ TCR (27). To validate that EPCR is expressed on MCs in vivo, we performed flow cytometry analysis on uninfected and DENV-infected draining LNs. Indeed, MCs expressed EPCR and there was a significant increase in the numbers of $EPCR^+$ MCs in draining LNs during DENV infection (**Figure 7G, S16A**). EPCR expression on MCs was also increased (**Fig. 7H, S16A-B**), whereas the numbers of $EPCR^+$ non-MCs and levels of EPCR on non-MCs were not significantly changed (**Figure 7H, S16C-D**). To determine if EPCR on MCs functionally affects γδ T cell activation during DENV infection, we also used si-RNA against *EPCR* (siRNA-EPCR) to determine if it could block MC-mediated DENV activation of γδ T cells, compared to scrambled control siRNA (siRNA-SC). No increase in cell activation was observed in γδ T cells co-cultured with BMMCs transfected with siRNA-EPCR (which showed a ~%83 knock-down, **Figure S17**), while siRNA-SC transfection of BMMCs did not inhibit γδ T cell activation resulting

from co-culture (**Figure 7I**). To confirm that EPCR is required for γδ T cell activation in vivo, we performed an experiment where a blocking and neutralizing antibody against EPCR was injected in FPs prior to infection with DENV. In support of the critical role of EPCR in γδ T cell activation during DENV infection, the numbers of both total (**Figure 7J**) and activated (**Figure 7K**) γδ T cells were reduced in LNs of animals that had been administered the EPCR-blocking antibody. These results show that EPCR is a critical component of the immune synapse between MCs and γδ T cells during DENV infection and that it promotes γδ T cell activation and proliferation.

Finally, to validate the importance of γδ T cells to the clearance of DENV infection in vivo, we infected γδ T cell-deficient mice (28) (γδ T-KO) with DENV and monitored the infection levels in the skin of the FP, the site of infection (**Figure 7L**) and LN (**Figure 7M**). Quantification of DENV by real time RT-PCR showed that viral burden was much higher in γδ T-KO mouse FPs at 24h post-infection compared to WT controls (**Figure 7L**). By 72h post-infection viral titers were higher in γδ T cell deficient mice in both the FP and the LN (**Figure 7L-M**). These results establish that γδ T cells contribute to clearance of DENV in vivo.

DISCUSSION

Although they both are responsible for surveillance at the front line of immune defense, MCs and γδ T cells have not been reported to interact with each other. This study demonstrates that antigen presentation by MCs to γδ T cells promotes γδ T cell activation in a TCR-dependent mechanism. In turn, γδ T cells promote the early and direct killing of virus-infected cells, as shown by the fact that γδ T cell-deficient animals have highly impaired clearance of virus from the site of infection and draining LNs.

At the initiation of inflammation to DENV in the skin, we observe MC-dependent recruitment of several subsets of T cells to the site of infection. This is consistent with previous studies that demonstrated the MC-dependent recruitment of NKT cells and $CD8^+$ T cells to sites

of viral infection (5). However, prior studies did not definitively ascribe the role of viral clearance to recruited T cells or reveal further mechanisms regarding how the newly-recruited cells could promote immunity. Taking a systematic approach to describe the subsets of T cells recruited to the DENV-infected skin, we identified that γδ T cells were the earliest responding T cell subset and that their recruitment is also MC-dependent. Since γδ T cells are known for patrolling the skin, we expected that their increased numbers in the tissue might only be due to local proliferation. Our results using CFSE labeling of local tissue-resident cells showed that this is only a partial explanation for the enrichment of γδ T cells in DENV-infected skin, since there is a substantial increase in the non-labelled portion of γδ T cells, which was suggestive of recruitment. However, a caveat to this interpretation is our observation that CFSE labelling in the tissue was not 100% and it is likely that proliferation of unlabeled cells could explain a portion of the increase in unlabeled cells, rather than solely recruitment. Adoptive transfer of CFSE labelled T cells to recipients prior to cutaneous DENV infection confirmed the recruitment of blood-derived T cells, including of the γδ subset, into the skin. Although it is important to acknowledge that CFSE labelling experiments have caveats(29), these labelling experiments in MC-deficient mice support that MCs induce both the recruitment and local proliferation of responding γδ T cells.

We observed that $\gamma\delta^+$, $CD8^+$ and NKT cells were all recruited in a MC-dependent fashion to the infected skin, while $CD4^+$ T cells were not substantially increased at early time points. This is likely because most $CD4^+$ T cells in the skin are T-regulatory cells, which would not be beneficial to the clearance of virus. In contrast, $CD4^+$ T cells are recruited abundantly in the draining LN during DENV infection, but most of those cells are traditional $\alpha\beta$ T helper cells. The influx of LN T cells is most likely the result of LN hypertrophy, which is dependent on MC-derived TNF (10). Further studies will be needed to define how MC contributions to LN hypertrophy shape downstream functions of $CD4^+$ T cells.

There are multiple indications in our data that MCs are more consequential to T cell recruitment than infected cells. First, we observe in Sash mice that there are higher levels of infection in the skin, but in spite of this there is greatly reduced recruitment of T cells at early time points. Second, even in trans-well experiments where infection-permissive cells were used, chemotaxis of T cells did not occur significantly as it did when MCs were activated on the opposite side of the trans-well. In spite of not showing direct chemotaxis towards infected macrophages, T cells are clearly still able to identify and kill infected cells, since levels of cytotoxicity increase in infected DCs compared to uninfected DCs in direct co-culture. MCs, in contrast, are not significant targets for T cell killing, likely due to the fact that they are very resistant to DENV infection (5). In spite of this, features of their activation are consistent with the process of abortive replication since they do apparently internalize virus particles and activation of MCs and cytokine production in response to DENV was previously shown to be dependent on cytosolic pattern recognition molecules such as TLR3 and MDA5 (5). These observations point to the conclusion that MCs act as immunosurveillance cells, promoting the recruitment and activation of T cells so that nearby infected cells can be targeted for killing.

Whether MCs are non-classical APCs has been debated. Some mechanisms have been postulated through which MCs could contribute indirectly to antigen presentation, for example by passing antigen to DCs for further processing and presentation (30), or by releasing exosomes that might come in contact with T cells and induce their activation (31). Multiple groups have observed that MCs and T cells can physically interact in tissues (16) and we previously observed that MCs interact with $CD3^+$ cells in DENV-infected skin (5), but it has not been clear if this interaction occurs as a component of the normal surveillance role of T cells in tissues (11). Several of our results presented here indicate that the interaction between MCs and γδ T cells is more analogous to “professional” antigen presentation rather than endogenous or “non-professional” antigen presentation. First, we observe that MCs and γδ T cells form conjugates in vivo that are characterized by polarization of the γδ TCR towards the MC contact

site. This indicates that immune synapses form, even though the MCs are not targets of killing, themselves. Second, we observe that a significant portion of the γδ T cell activation and proliferation occurs only in the presence of DENV. Third, T cell activation is dependent on TCR signaling cascades. This is shown by the observation that the ERK-pathway inhibitor, which was used to block TCR activation, completely abrogates the antigen-dependent component of γδ T cell activation. Like other groups (11), we also saw a certain amount of non-specific γδ T cell activation that was MC-contact dependent. While there is a baseline increase in T cell activation upon co-culture with MCs, this is likely due to secretion of soluble factors including leukotrienes since a portion of the response is inhibited by the leukotriene receptor antagonist montelukast. Other studies also show that soluble factors released by MCs, including TNF, can contribute to increased basal T cell activation (32), although in our co-culture TNF blockade did not affect the basal activation levels. It should also be noted that we observed antigen-specific activation of traditional $\alpha\beta$ $CD4^+$ and $CD8^+$ T cells, which is also suggestive of traditional antigen presentation by MCs and warrants future exploration of the functional consequences to immunity. Here, we focused on identifying the mechanism of TCR-dependent activation of γδ T cells by MCs. Pull-down of the γδ TCR revealed that it is physically associated with the non-classical antigen presentation molecule, EPCR. Other studies have also previously shown that EPCR is a ligand for γδ TCR, which suggested it could be a ligand for infected or stressed cells (27). Interestingly, the EPCR molecule binds the phospholipid phosphatidylethanolamine (33), which is present on DENV particles, likely derived from the ER membrane that is used for virus budding (34). Blocking of EPCR in MCs, either with siRNA or with a neutralizing antibody, was also shown to significantly prevent γδ T cell activation both in vitro and in vivo. Our data suggest that the interaction of these molecules is critical for γδ T cell activation, but there may be other molecules that could participate in the interaction between MCs and γδ T cells that are also important.

Although γδ T cells have been shown in some cases to bind to viral glycoproteins, resulting in direct activation, independent of antigen presentation, we observe that DENV alone has minimal influence on γδ T cells and did not result in significant levels of activation. Our results also indicated that $CD4^+$ T cells, even though not recruited by MCs significantly to sites of DENV infection, expand in co-culture in the presence of MCs. This suggests that MCs are also able to activate $CD4^+$ cells in an antigen-dependent manner, but it is not clear from this data whether this would occur in vivo since there are very few MCs in draining LNs where $CD4^+$ T cells are abundant and those there are primarily confined to the LN sinuses (35, 36), segregated away from T cell zones. Future studies are needed to understand the molecules that are used by MCs to present antigen to conventional T cells.

Activation of γδ T cells by MCs involves upregulation of the activation marker CD69 and proliferation, which is shown to be MC-dependent. Consistent with these findings, IFN-γ production, another indicator of γδ T cell activation, was absent in Sash mice in the γδ T cell subset. It is also interesting to note, from the context of DENV immune defense, that γδ T cells were the primary T cell subset that produced IFN-γ during early time points of infection. Using γδ T cell-deficient mice we also confirmed that the MC-initiated and -dependent recruitment of γδ T cells is physiologically relevant during peripheral viral infection since γδ T-KO animals had higher viral titers at the site of infection and in secondary target organs. This is consistent with prior studies showing that γδ T cells are important for clearance of West Nile virus (19, 20), which is closely related to DENV. Interestingly, since the DENV replication cycle requires approximately 12h for completion, our evidence that γδ T cells promote lower virus titers within 24h of infection emphasize that they are capable of responding to infection and killing target cells that have been infected within the first or second amplification cycles of the virus in vivo. This contrasts the role of MCs we have observed previously during systemic infection, where wide-spread activation of MCs can contribute significantly to inducing vascular leakage and pathological signs of DENV disease (37). Prior to systemic infection, early MC activation is

protective, having the potential to significantly limit the infection burden in vivo through the recruitment and activation of T cells. Together, our results define a new role for MCs as non-conventional APCs in peripheral tissues that are responsible for the recruitment and TCR-mediated activation of γδ T cells, leading to viral infection clearance.

EXPERIMENTAL PROCEDURES

Animal studies. All animal experiments were conducted in the vivarium at Duke-NUS Medical School. C57BL/6 mice were purchased from InVivos (Singapore). MC-deficient mice (W^{sh}/W^{sh}; 'Sash') and γδ T cell-deficient mice (B6.129P2-*Tcrd*^{tm1Mom}/J) were originally purchased from Jackson Laboratories and bred in-house. Mcpt5-Cre/iDTR mice were generated by crossing Mcpt5-Cre mice (provided by Prof. Axel Roers, Dresden University, Dresden, Germany) to a Cre excision reporter strain, iDTR (C57BL/6-*Gt(ROSA)26Sor*$^{tm1(HBEGF)Awai}$/J), from Jackson Laboratories. For all strains, 6-8 weeks old female mice were used for the experiments.

Infections. For infections, Eden2, a clinical isolate of DENV2 was used. This low-passage clinical isolate was originally obtained from the Duke-NUS reference laboratory and derived from the clinical study (Early Dengue Infection and Outcomes Study, Eden)(38). Virus strains were propagated in *Aedes albopictus* C6/36 mosquito cells (CRL-1660; ATCC), maintained in RPMI medium 1640 with 25 mM HEPES, and titered using standard methods (5, 39). Mice were infected with 1×10^5 pfu of DENV subcutaneously in FPs or by intraperitoneal injection of 1×10^6 PFU of DENV. Sash mice were intravenously injected with $1x10^7$ mature BMMCs from congenic controls to generate reconstituted Sash (Sash-R), mice as previously described(5). Mcpt5-Cre/iDTR mice were injected with DT (25ng/g bodyweight) every week for 4 weeks for systemic MC depletion before infection following a published protocol (24). Depletion efficiency was assessed by flow cytometry. For in vivo labeling of T cells 1×10^{-6} mmols of CellTrace™ CFSE

(Thermo Fisher Scientific) was injected subcutaneously in FPs 4h prior to infection with DENV, according to an established protocol(9). To verify the migration of blood-derived cells into FPs and LNs, splenocytes from mice were labelled *ex vivo* with CellTrace™ CFSE at a final concentration of 5μM after lysis of RBCs. CFSE labelled splenocytes ($1x10^7$) were then adoptively transferred to recipient mice by tail vein injection. In vivo blocking of EPCR (ThermoFisher Scientific, 16-2012-83) was achieved by subcutaneous injection of 5μg of monoclonal antibody at 24h and 4h prior to infection. For controls, an IgG isotype control (ThermoFischer Scientific, 16-4031-81) was similarly injected prior to infection.

Flow Cytometry. FP skin and popliteal LNs were harvested and dissociated with collagenase (Sigma) before passing through a cell strainer (BD Biosciences) to make single cell suspensions. Total cell numbers were determined by counting with a hemocytometer. Cells were then stained with anti-CD45-BUV395 (564279), anti-CD3e-PercP-Cy5.5 (551163), anti-CD4-BV650 (563232), anti-CD8a-Alexa700 (557959), anti-CD69-FITC (557392), anti-CD25-BV785 (564023) (all from BD Biosciences), anti-NK1.1-PE (eBiosciences,12-5941-82) and anti-γδ TCR-APC (BioLegend, 118116). Depletion of MCs in skin and peritoneum was confirmed by staining the cells from FP and peritoneal lavage with anti-CD45-BUV395, anti-c-kit-APC (eBiosciences, 17-1171-82) and anti-FcεR1α-PE (Invitrogen, 12-5898-82). Expression of EPCR on MCs in LNs was measured by staining cells with anti-c-Kit-PE-CY7(105814), anti- FcεR1α-PE (134308) and anti-EPCR-APC (141506) antibodies (all from Biolegend). For intracellular IFN-γ staining (using anti-IFN-γ-BV711, BD Biosciences, 564336), cells were first incubated with 2μM monensin (BioLegend) for 6h at 37°C. Intracellular staining for CXCL10 (701225) and CCL2 (12-7096-81) was performed with similar methods in BMMCs, using antibodies from ThermoFisher Scientific. Flow cytometry data were acquired with a LSRFortessa™ cell analyzer (BD Biosciences) and analyzed using FlowJo software (FlowJo, LLC).

Virus quantification. DENV genomic copy numbers in the FPs and LNs were quantified by homogenizing tissues in tissue lysis buffer (Buffer RLT; Qiagen) with ceramic beads (Glen Mills) using a mechanical homogenizer (Qiagen). Total RNA was isolated using the RNeasy kit (Qiagen) according to the manufacturer's protocol. cDNA was synthesized using the iScript cDNA Synthesis Kit (Bio-Rad), with 5 pmole of a DENV2 primer added to the reaction mix. DENV2-forward and DENV2-reverse primers (**Table S1**) were used for quantification using SYBR Green reagent (Bio-Rad) in a CFX96 Touch Real-Time PCR Detection System (Bio-Rad). Copy numbers were then calculated using a DENV standard curve generated from serial dilutions of a DNA plasmid containing the DENV genomic sequence.

Transwell and Co-culture Assays. To generate BMMCs, bone marrow was flushed from naïve C57BL/6 mouse femurs and cultured in RPMI medium containing 10% FBS, 1% supernatant from Cho-KL cells which contains stem cell factor (produced in house), penicillin and streptomycin, HEPES, trypsin inhibitor, sodium pyruvate (Thermo Fisher Scientific), and recombinant IL-3 (5 ng/ml, R&D Systems). After 4 weeks, MCs were verified to be >95% pure by toluidine blue (Sigma-Aldrich) staining prior to use. BMMΦ were prepared as described elsewhere (40). T cells were purified from LNs of naïve C57BL/6 mouse using Pan T cell isolation kit II mouse (Miltenyi Biotec), according to manufacturer's instructions. For trans-well migration assays, 1×10^5 T cells were applied to trans-well inserts with 3-μm pores (BD-Biosciences) and 1×10^5 BMMC or BMMΦ were grown in the lower chamber in a 24 well plate. Cells were infected using MOI 1 of DENV2 for 1h in the lower chamber prior to putting the inserts and adding T cells to the top chamber of the trans-well. T cell numbers in the upper chamber were counted after 12h and subtracted from the initial count to determine the number of T cells that migrated to the bottom chamber. Flow cytometry was used to characterize the subsets of T cells that migrated to the bottom chamber.

For co-culture assays, 1×10^5 BMMC were mixed with 1×10^5 T cells in complete RPMI with 20U/ml mIL-2 (Sigma) for 48-96h. To challenge BMMCs with DENV2, BMMCs were incubated with DENV (MOI=1) for 1h prior to co-culture. Flow cytometry was used to characterize the frequency of T cells after co-culture. MEK162 (Selleckchem) was used at a concentration of 0.2μM for the inhibition assay.

For si-RNA mediated knock down of BMMCs, BMMCs were transfected with 200nM EPCR si-RNA or scrambled control (Santa Cruz Biotechnology) using 4D-Nucleofector (Lonza). Knock-down efficiency was checked 24h post transfection using the primers provided by Santa Cruz in the siRNA kit. These cells were then co-cultured with T cells for 72h before measuring the effect of EPCR knockdown on γδ T cell activation.

Cytotoxicity and Proliferation Assays. A LDH cytotoxicity assay (Thermo Fisher Scientific) was used to assess the ability of γδ T cells to lyse DENV-infected DCs following manufacturer's instructions. To assess the cytotoxicity ability of activated γδ T cells *ex vivo*, T cells were isolated from the LNs of DENV2 infected mice 72h post infection using the Miltenyi Pan T cell isolation kit II mouse (Miltenyi Biotec). γδ T cells were then depleted from total T cells using TCR $\gamma\delta^+$ T Cell Isolation Kit mouse (Miltenyi Biotec). Cytotoxicity ability of γδ T cells was inferred by comparing the cytotoxicity activity of total T cells and γδ-depleted T cells. BMDCs were prepared as described elsewhere (41). BMMCs and BMDCs were exposed to DENV2 (MOI=2) for 24h prior to co-culture with T cells or γδ-depleted T cells to measure cytotoxicity. In addition to the LDH assay, BMDCs treated in the aforementioned way were also stained with Annexin-V-FITC and propidium iodide (PI), 24h post co-culture and cytotoxicity was measured by determining the percentage of Annexin-V^+ and PI^+ BMDCs. For measuring T cell proliferation, T cells were first labeled with CellTrace CFSE (Thermo Fisher Scientific) according to the manufacturer's instructions, prior to co-culture with BMMC, with and without DENV2 (MOI=1). Viability was assayed using LIVE/DEAD™ Fixable Near-IR Dead Cell Stain Kit

(ThermoFisher Scientific) according to manufacturer's instructions. Proliferation was measured by dilution of CFSE in live γδ T cells by flow cytometry.

Chemokine expression analysis. BMMCs were challenged with DENV2 (MOI=1) and cells were harvested after 3h, 6h, 12h and 24h. Total RNA was isolated using the RNeasy kit (Qiagen) according to the manufacturer's instructions. Expression of chemokines (*CCL2*, *CCL20*, *CCL25*, *CCL27*, *CXCL10*) were then determined using primers listed in Table S1. The relative expression was calculated by normalizing to the expression of GAPDH and actin using the Bio-Rad CFX 3.1 software.

Immunofluorescence microscopy. FPs were frozen in OCT compound (Tissue-Tek), and frozen-sectioned (10 μm thick) using a cryostat (Leica). Sections were acetone fixed at 4°C, then blocked with PBS containing 1% BSA prior to staining with primary antibodies: anti-CD31 (BD Biosciences), anti-γδTCR (BioLegend, 118101) and avidin-TRITC (Thermo Fisher Scientific). Secondary antibodies used were anti-rat-Dy405 (Abcam, ab175671) and anti-hamster-AF647 (Thermo Fisher Scientific, A21451). For staining of peritoneal cells, cells were first cytospun on to glass slides before fixing with acetone. Primary antibodies used were anti-CD3-FITC (Thermo Fisher Scientific, HM3501), anti-γδTCR-APC (Biolegend, 118116), anti-tubulin (ThermoFisher Scientific, MA1-80017) and avidin-TRITC. The secondary antibody for tubulin staining was anti-mouse AF405 (Abcam, ab175658). Slides were mounted with Prolong gold antifade reagent (Thermo Fisher Scientific) and images were acquired using a Carl Zeiss LSM710 confocal microscope. Images show single optical sections acquired in channel-series. Merged images contain all channels and co-localization images were generated using ImageJ software.

Immunoprecipitation assay. Total T cells isolated from naïve mice were depleted of $CD4^+$ and $CD8^+$ T cells using microbeads (Miltenyi). The remaining T cells were then co-cultured with BMMCs exposed to MOI 1 of DENV2 for 1h at a 1:5 ratio. Cells were pelleted after 24h and washed twice with cold PBS. Cells were then lysed in RIPA buffer with 1x protease inhibitor cocktail. Cell lysates precleared with Protein A/G Agarose beads (ThermoFisher Scientific) were then incubated O/N with 2µg of anti-γδTCR antibody (BioLegend, 118101) or isotype antibody (BioLegend, 400901) in the cold room, followed by incubation with Protein A/G Agarose beads for 6h. Beads were washed 3 times with lysis buffer and protein complexes were fractioned by SDS-PAGE. Proteins were detected on western blots with polyclonal anti-γTCR (Santa Cruz Biotechnology, SC-25609) and anti-EPCR (ThermoFisher Scientific, PA5-32217) antibodies.

Statistical analysis. Unpaired two-tailed Student's t-tests or 1-way or 2-way ANOVA, were used, as appropriate, to determine statistical significance, in Excel or Prism software. $P \leq 0.05$ was considered significant. Error bars represent the SEM.

Study Approval. All animal experiments were performed according to protocols approved by SingHealth Institutional Animal Care and Use Committee.

SUPPLEMENTAL INFORMATION

Supplemental Figures and Table accompany this manuscript.

AUTHOR CONTRIBUTIONS

Experiments were primarily performed by CKM. Both authors contributed to experimental design, data analysis and interpretation. ALS conceived the study and wrote the manuscript. CKM reviewed the manuscript and contributed to its revision.

ACKNOWLEDGMENTS

We thank Abhay Rathore for discussions and critical manuscript review and Axel Roers for permission to use MCPT5-cre mice for this study. This work was funded by NMRC/CBRG/0084/2015 and start-up funding from Duke-NUS Medical School.

REFERENCES

1. Abraham SN, and St John AL. Mast cell-orchestrated immunity to pathogens. *Nat Rev Immunol.* 2010;10(6):440-52.

2. Galli SJ, Nakae S, and Tsai M. Mast cells in the development of adaptive immune responses. *Nat Immunol.* 2005;6(2):135-42.

3. Tsai M, Grimbaldeston M, and Galli SJ. Mast cells and immunoregulation/immunomodulation. *Adv Exp Med Biol.* 2011;716(186-211.

4. St John AL, and Abraham SN. Innate immunity and its regulation by mast cells. *J Immunol.* 2013;190(9):4458-63.

5. St John AL, Rathore AP, Yap H, Ng ML, Metcalfe DD, Vasudevan SG, and Abraham SN. Immune surveillance by mast cells during dengue infection promotes natural killer (NK) and NKT-cell recruitment and viral clearance. *Proc Natl Acad Sci U S A.* 2011;108(22):9190-5.

6. Orinska Z, Bulanova E, Budagian V, Metz M, Maurer M, and Bulfone-Paus S. TLR3-induced activation of mast cells modulates CD8+ T-cell recruitment. *Blood.* 2005;106(3):978-87.

7. Ebert S, Becker M, Lemmermann NA, Buttner JK, Michel A, Taube C, Podlech J, Bohm V, Freitag K, Thomas D, et al. Mast cells expedite control of pulmonary murine cytomegalovirus infection by enhancing the recruitment of protective CD8 T cells to the lungs. *PLoS Pathog.* 2014;10(4):e1004100.

8. Kunder CA, St John AL, and Abraham SN. Mast cell modulation of the vascular and lymphatic endothelium. *Blood.* 2011;118(20):5383-93.

9. Shelburne CP, Nakano H, St John AL, Chan C, McLachlan JB, Gunn MD, Staats HF, and Abraham SN. Mast cells augment adaptive immunity by orchestrating dendritic cell trafficking through infected tissues. *Cell Host Microbe.* 2009;6(4):331-42.

10. McLachlan JB, Hart JP, Pizzo SV, Shelburne CP, Staats HF, Gunn MD, and Abraham SN. Mast cell-derived tumor necrosis factor induces hypertrophy of draining lymph nodes during infection. *Nat Immunol.* 2003;4(12):1199-205.

11. Kambayashi T, and Laufer TM. Atypical MHC class II-expressing antigen-presenting cells: can anything replace a dendritic cell? *Nat Rev Immunol.* 2014;14(11):719-30.

12. Nakae S, Suto H, Iikura M, Kakurai M, Sedgwick JD, Tsai M, and Galli SJ. Mast cells enhance T cell activation: importance of mast cell costimulatory molecules and secreted TNF. *J Immunol.* 2006;176(4):2238-48.

13. Mor A, Shefler I, Salamon P, Kloog Y, and Mekori YA. Characterization of ERK activation in human mast cells stimulated by contact with T cells. *Inflammation.* 2010;33(2):119-25.

14. Frandji P, Oskeritzian C, Cacaraci F, Lapeyre J, Peronet R, David B, Guillet JG, and Mecheri S. Antigen-dependent stimulation by bone marrow-derived mast cells of MHC class II-restricted T cell hybridoma. *J Immunol.* 1993;151(11):6318-28.

15. Hong GU, Kim NG, Kim TJ, and Ro JY. CD1d expressed in mast cell surface enhances IgE production in B cells by up-regulating CD40L expression and mediator release in allergic asthma in mice. *Cell Signal.* 2014;26(5):1105-17.

16. Mekori YA, and Metcalfe DD. Mast cell-T cell interactions. *J Allergy Clin Immunol.* 1999;104(3 Pt 1):517-23.

17. Vantourout P, and Hayday A. Six-of-the-best: unique contributions of gammadelta T cells to immunology. *Nat Rev Immunol.* 2013;13(2):88-100.

18. Bonneville M, O'Brien RL, and Born WK. Gammadelta T cell effector functions: a blend of innate programming and acquired plasticity. *Nat Rev Immunol.* 2010;10(7):467-78.

19. Wang T, Scully E, Yin Z, Kim JH, Wang S, Yan J, Mamula M, Anderson JF, Craft J, and Fikrig E. IFN-gamma-producing gamma delta T cells help control murine West Nile virus infection. *J Immunol.* 2003;171(5):2524-31.

20. Wang T, Gao Y, Scully E, Davis CT, Anderson JF, Welte T, Ledizet M, Koski R, Madri JA, Barrett A, et al. T Cells Facilitate Adaptive Immunity against West Nile Virus Infection in Mice. *The Journal of Immunology.* 2006;177(3):1825-32.

21. Jutila MA, Holderness J, Graff JC, and Hedges JF. Antigen-independent priming: a transitional response of bovine gammadelta T-cells to infection. *Anim Health Res Rev.* 2008;9(1):47-57.

22. Reber LL, Marichal T, and Galli SJ. New models for analyzing mast cell functions in vivo. *Trends Immunol.* 2012;33(12):613-25.

23. Bousso P. T-cell activation by dendritic cells in the lymph node: lessons from the movies. *Nat Rev Immunol.* 2008;8(9):675-84.

24. Dudeck A, Dudeck J, Scholten J, Petzold A, Surianarayanan S, Kohler A, Peschke K, Vohringer D, Waskow C, Krieg T, et al. Mast cells are key promoters of contact allergy that mediate the adjuvant effects of haptens. *Immunity.* 2011;34(6):973-84.

25. Kohno M, and Pouyssegur J. Targeting the ERK signaling pathway in cancer therapy. *Ann Med.* 2006;38(3):200-11.

26. Kusters-Vandevelde HV, Willemsen AE, Groenen PJ, Kusters B, Lammens M, Wesseling P, Djafarihamedani M, Rijntjes J, Delye H, Willemsen MA, et al. Experimental treatment of NRAS-mutated neurocutaneous melanocytosis with MEK162, a MEK-inhibitor. *Acta Neuropathol Commun.* 2014;2(41.

27. Willcox CR, Pitard V, Netzer S, Couzi L, Salim M, Silberzahn T, Moreau JF, Hayday AC, Willcox BE, and Dechanet-Merville J. Cytomegalovirus and tumor stress surveillance by binding of a human gammadelta T cell antigen receptor to endothelial protein C receptor. *Nat Immunol.* 2012;13(9):872-9.

28. Itohara S, Mombaerts P, Lafaille J, Iacomini J, Nelson A, Clarke AR, Hooper ML, Farr A, and Tonegawa S. T cell receptor delta gene mutant mice: independent generation of alpha beta T cells and programmed rearrangements of gamma delta TCR genes. *Cell.* 1993;72(3):337-48.

29. Ganusov VV, Pilyugin SS, de Boer RJ, Murali-Krishna K, Ahmed R, and Antia R. Quantifying cell turnover using CFSE data. *J Immunol Methods.* 2005;298(1-2):183-200.

30. Carroll-Portillo A, Cannon JL, Te Riet J, Holmes A, Kawakami Y, Kawakami T, Cambi A, and Lidke DS. Mast cells and dendritic cells form synapses that facilitate antigen transfer for T cell activation. *J Cell Biol.* 2015;210(5):851-64.

31. Skokos D, Le Panse S, Villa I, Rousselle JC, Peronet R, David B, Namane A, and Mecheri S. Mast cell-dependent B and T lymphocyte activation is mediated by the secretion of immunologically active exosomes. *J Immunol.* 2001;166(2):868-76.

32. Nakae S, Suto H, Kakurai M, Sedgwick JD, Tsai M, and Galli SJ. Mast cells enhance T cell activation: Importance of mast cell-derived TNF. *Proc Natl Acad Sci U S A.* 2005;102(18):6467-72.

33. Chiappori F, Merelli I, Milanesi L, and Rovida E. Exploring the role of the phospholipid ligand in endothelial protein C receptor: a molecular dynamics study. *Proteins.* 2010;78(12):2679-90.

34. Carnec X, Meertens L, Dejarnac O, Perera-Lecoin M, Hafirassou ML, Kitaura J, Ramdasi R, Schwartz O, and Amara A. The Phosphatidylserine and Phosphatidylethanolamine Receptor CD300a Binds Dengue Virus and Enhances Infection. *J Virol.* 2016;90(1):92-102.

35. Tedla N, Wang HW, McNeil HP, Di Girolamo N, Hampartzoumian T, Wakefield D, and Lloyd A. Regulation of T lymphocyte trafficking into lymph nodes during an immune response by the chemokines macrophage inflammatory protein (MIP)-1 alpha and MIP-1 beta. *J Immunol.* 1998;161(10):5663-72.

36. Kurashige C, Hashimoto T, and Hatai B. Mast cells in the lymphnode sinus of the rat. *Arch Histol Jpn.* 1966;27(1):345-50.

37. St John AL. Influence of mast cells on dengue protective immunity and immune pathology. *PLoS Pathog.* 2013;9(12):e1003783.

38. Low JG, Ooi EE, Tolfvenstam T, Leo YS, Hibberd ML, Ng LC, Lai YL, Yap GS, Li CS, Vasudevan SG, et al. Early Dengue infection and outcome study (EDEN) - study design and preliminary findings. *Ann Acad Med Singapore.* 2006;35(11):783-9.

39. Schulze IT, and Schlesinger RW. Plaque assay of dengue and other group B arthropod-borne viruses under methyl cellulose overlay media. *Virology.* 1963;19(40-8.

40. Zhang X, Goncalves R, and Mosser DM. The isolation and characterization of murine macrophages. *Curr Protoc Immunol.* 2008;Chapter 14(Unit 14 1.

41. Madaan A, Verma R, Singh AT, Jain SK, and Jaggi M. A stepwise procedure for isolation of murine bone marrow and generation of dendritic cells. *2014.* 2014.

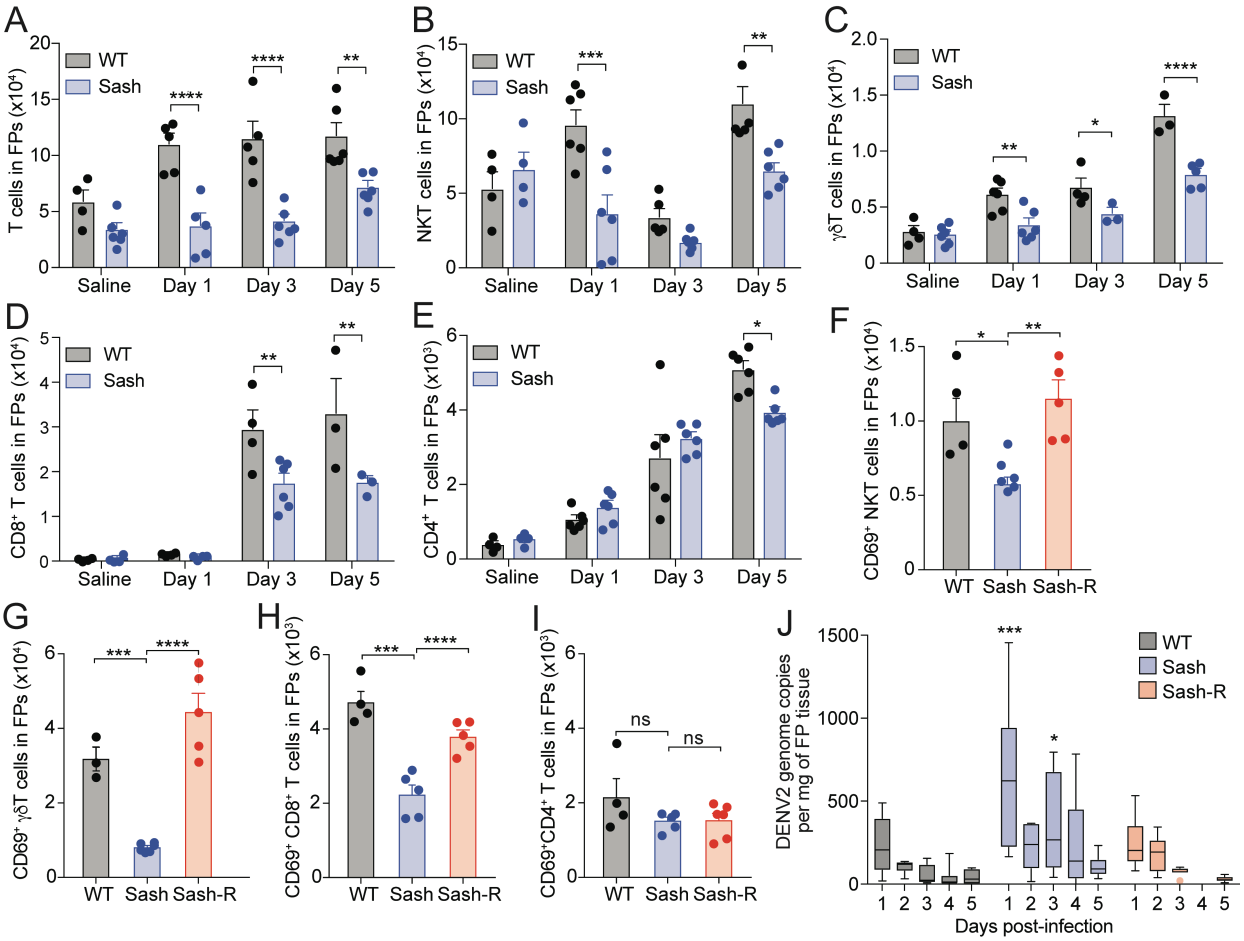

Figure 1: MC-dependent recruitment and activation of T cells in the skin during DENV infection. MC-deficient (Sash) and MC-sufficient (WT) mice were injected with saline or infected with 1×10^5 pfu DENV by subcutaneous injection in FP to determine if T cells were recruited in a MC-dependent fashion during infection. FP skin was collected on days 1, 3, and 5 post-infection and dissociated with collagenase to make single cell suspensions, which were stained for various subsets of T cells prior to flow cytometry (**Figure S1**). Numbers of (**A**) Total T cells ($CD3^+$) (**B**) NKT cells ($CD3^+NK1.1^+$) (**C**) γδ T cells ($CD3^+\gamma\delta TCR^+$) (**D**) $CD8^+$ T cells ($CD3^+CD8^+$) and (**E**) $CD4^+$ T cells ($CD3^+CD4^+$) were compared between WT and Sash mice. Sash mice reconstituted with BMMCs (Sash-R) were similarly infected and FP skin cells were stained on day 3 post infection. Reconstitution of MCs in Sash mice restored the deficiency in T cell numbers (**Figure S2A-E**). For multiple T cell subsets, (**F**) NKT (**G**) γδ T and (**H**) $CD8^+$ T cells, (**I**) but not $CD4^+$ T cells, there were greater numbers of activated ($CD69^+$) T cells in FP in WT mice compared to Sash mice day 3 post-infection and the deficiency in activation was repaired in Sash-R mice. (**J**) Greater genome copies of DENV were detected in the FP of Sash mice compared to WT mice and Sash-R, as determined by RT-PCR. Means are depicted by box and whisker plots with Tukey's test error bars. An alternate presentation of the data in panel (**J**) showing individual mouse values is provided in **Figure S2F**. For all panels unless otherwise noted, data represent mean ± SEM; *p<0.05, **p<0.001, ***p<0.001 by 2-way ANOVA (Sidak's multiple comparison test), n=4-6 mice. Reduced recruitment and activation of several subsets of T cells occurred in the skin of MC-deficient mice during DENV infection which was repaired upon reconstitution of MC-deficient mice with MCs.

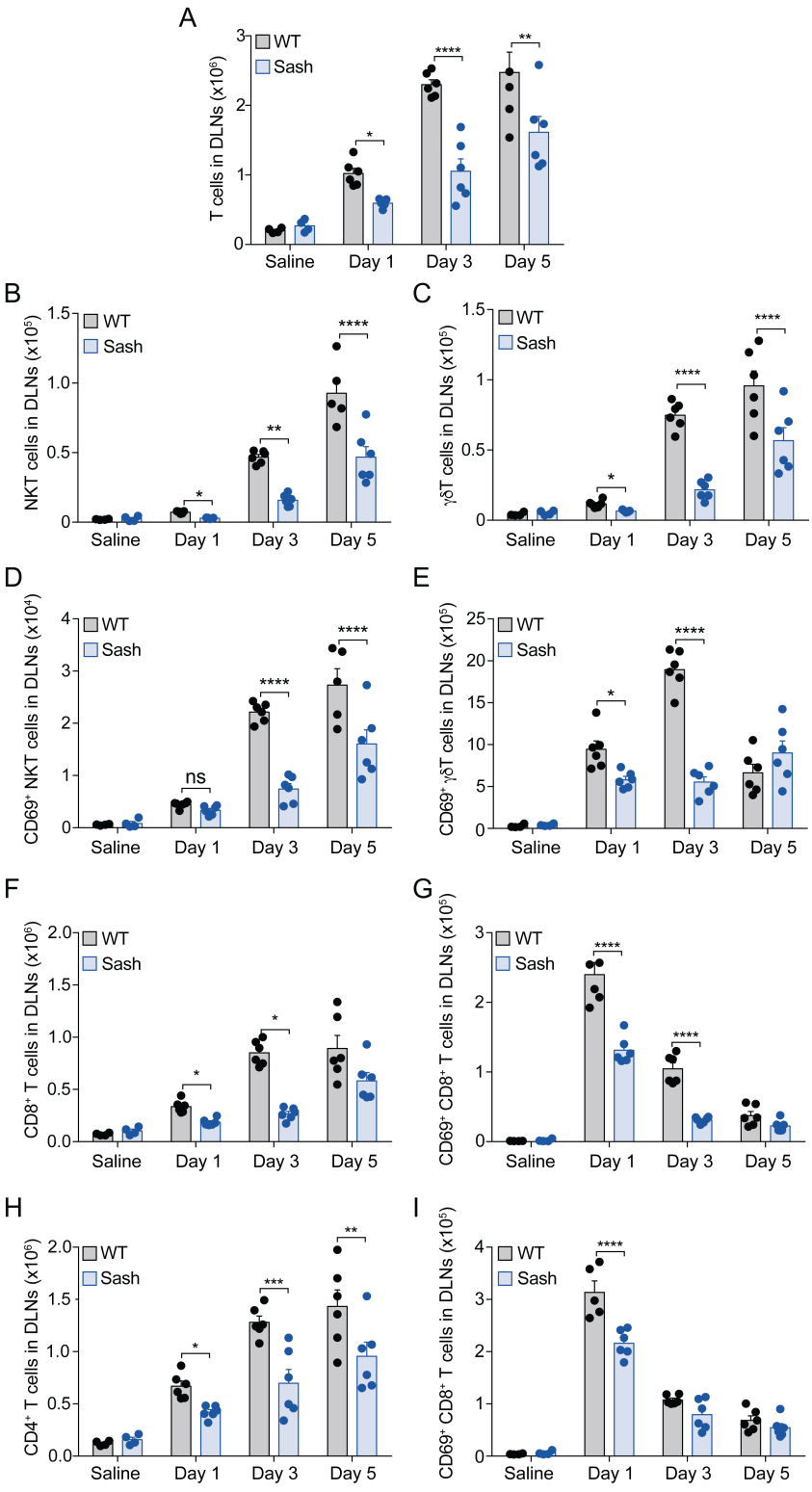

Figure 2: Reduced retention of multiple subsets of T cells in the draining LN and reduced T cell activation in MC-deficient mice. Mice were injected with saline or infected with 1×10^5 pfu of DENV via FP and popliteal LNs were collected on days 1, 3 and 5 post-infection. LNs were dissociated to make single cell suspensions and cells were stained with antibodies against

CD45, CD3, CD4, CD8, NK1.1, γδ TCR and CD69. (**A**) Total T cells ($CD3^+$) (**B**) NKT cells ($CD3^+NK1.1^+$) (**C**) γδ T cells ($CD3^+\gamma\delta TCR^+$) (**D**) activated NKT cells ($CD3^+NK1.1^+CD69^+$) (E) activated γδ T cells ($CD3^+\gamma\delta TCR^+CD69^+$) (F) $CD8^+$ T cells ($CD3^+CD8^+$) (**G**) activated $CD8^+$ T cells ($CD3^+CD8^+CD69^+$) (H) $CD4^+$ T cells ($CD3^+CD4^+$) and activated $CD4^+$ T cells ($CD3^+CD4^+CD69^+$) were compared between WT and Sash mice. Data represent mean ± SEM, *p<0.05,**p<0.01, ****p<0.0001 by 2-way ANOVA (Sidak's multiple comparison test) and n=4-6 mice per group. MC-deficient mice have defects in recruitment and activation of multiple T cell subsets to draining LNs.

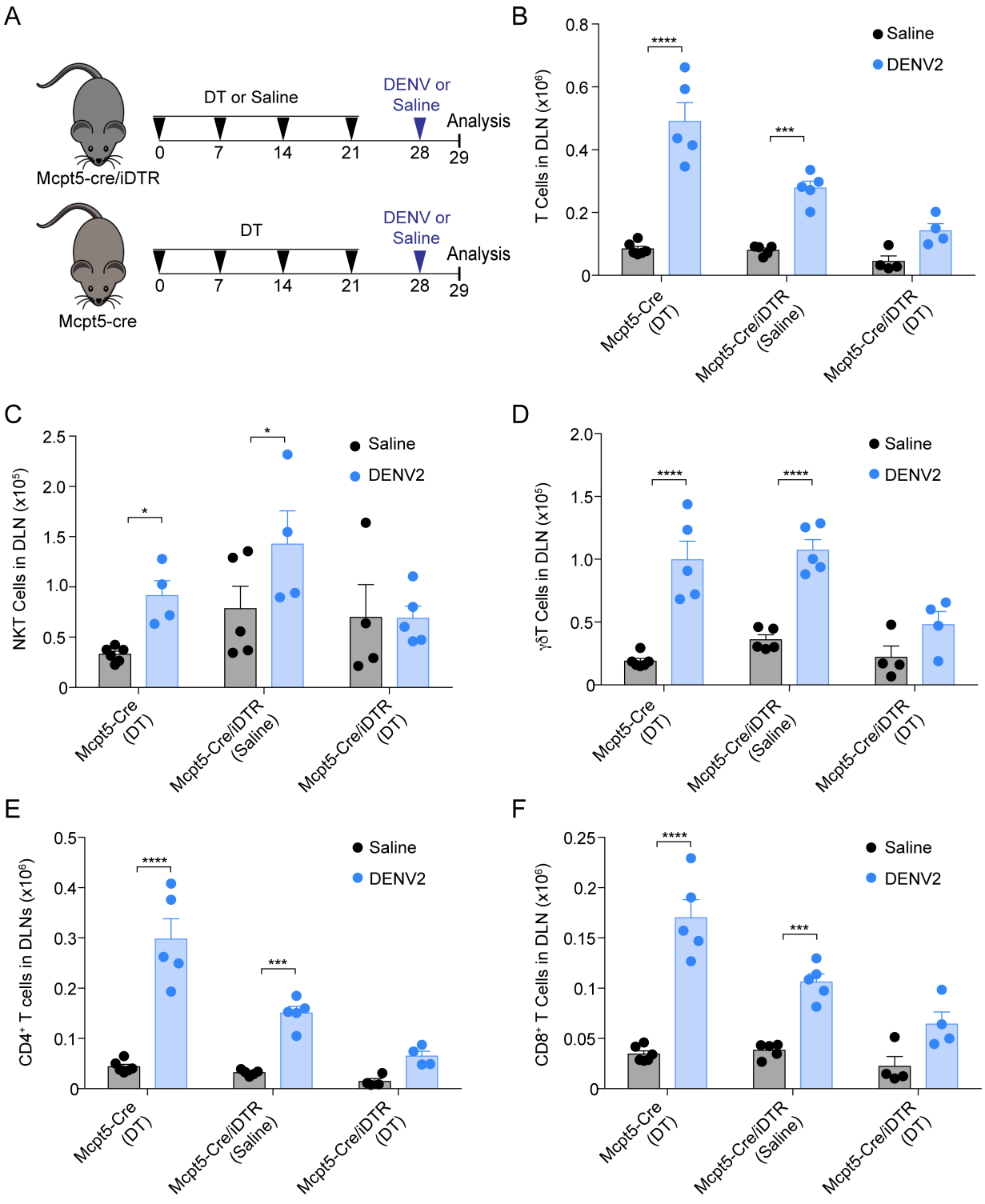

Figure 3. Defects in T cell recruitment to DENV-infected LNs in the MCPT5-cre iDTR model of MC deficiency. (**A**) Schematic showing timeline for DT and DENV injection. Mcpt5-Cre and Mcpt5-Cre/iDTR were injected with saline to serve as control or diphtheria toxin every week for 4 weeks for systemic MC depletion before infection. Mice were injected with saline or infected with 1×10^5 pfu DENV subcutaneously in FP and the popliteal LNs were collected 24h post-infection. Single cell suspensions of LNs were stained to identify T cell subsets using the

gating strategy in **Figure S1**. T cell responses to DENV infection were compared between MC-sufficient Mcpt5-Cre/iDTR (saline-injected), MC-sufficient MCPT5-cre (DT-injected) and MC-deficient Mcpt5-Cre/iDTR (DT-injected) mice. (**B**) Total T ($CD3^+$) (**C**) NKT ($CD3^+NK1.1^+$) (**D**) γδ T ($CD3^+$γδ TCR^+) (**E**) $CD4^+$ T cells ($CD3^+CD4^+$) and (**F**) $CD8^+$ T ($CD3^+CD8^+$) all showed MC-dependent recruitment to LNs during DENV infection in this *ckit*-independent model of MC deficiency. Data represent mean ± SEM ; * $p < 0.05$, ** $p < 0.01$, *** $p < 0.001$, **** $p < 0.0001$ by 2-way ANOVA (with Sidak's multiple comparison test) with n=4-6 animals per group. Efficiency of MC depletion post injection with DT is shown in **Figure S4**.

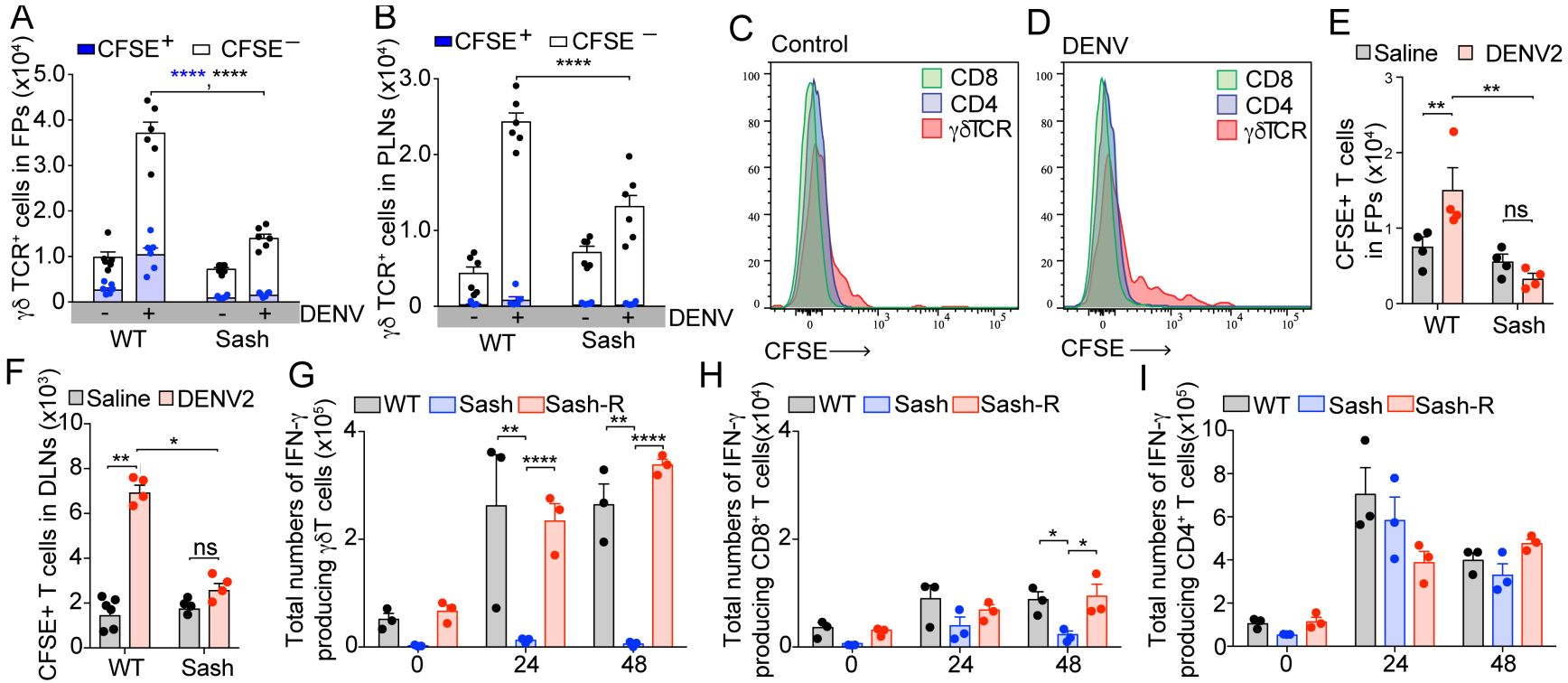

Figure 4: MC-dependent recruitment, proliferation and activation of γδ T cells at sites of DENV infection. WT and Sash mice were injected with CFSE, 4h prior subcutaneous FP injection with 1×10^5 pfu of DENV or saline. (**A**) FP and (**B**) draining LNs were collected at 24h post-infection and $CFSE^+$ and $CFSE^-$ γδ T cells were enumerated by flow cytometry. Sash mice showed significantly reduced numbers of both $CFSE^+$ and $CFSE^-$ γδT cells in FPs compared to WT mice. Representative histograms showing CFSE detection in $CD4^+$, $CD8^+$, and γδT cell subsets in the draining LN of (**C**) uninfected and (**D**) infected WT mice. γδT cells but not $CD4^+$ or $CD8^+$ T cells migrated to the draining LN from the site of infection. Multiple peaks in the histogram indicate proliferation of γδ T cells. Recruitment of T cells was observed in the (**E**) FP and (**F**) LN upon infection in WT but not Sash mice was confirmed by injecting CFSE labelled splenocytes 24h prior to infection and analyzing the $CFSE^+$ T cell numbers in FPs and LNs 24h post-infection. (**G-I**) Single cell suspensions of LNs, collected at 24h and 48h post infection were treated with monensin for 6h and then stained for surface markers CD3, CD4, CD8, γδ TCR and intracellularly for IFN-γ. Total numbers of IFN-γ producing cells in WT, Sash and Sash-R mice were subtyped based on (**G**) γδ (**H**) $CD8^+$ and (**I**) $CD4^+$ T cells. For all panels, Data represent mean ± SEM. *p<0.05, ** p<0.01 ****p<0.0001 by two-way ANOVA (Sidak's multiple comparison test) and n=3-6 mice per group.

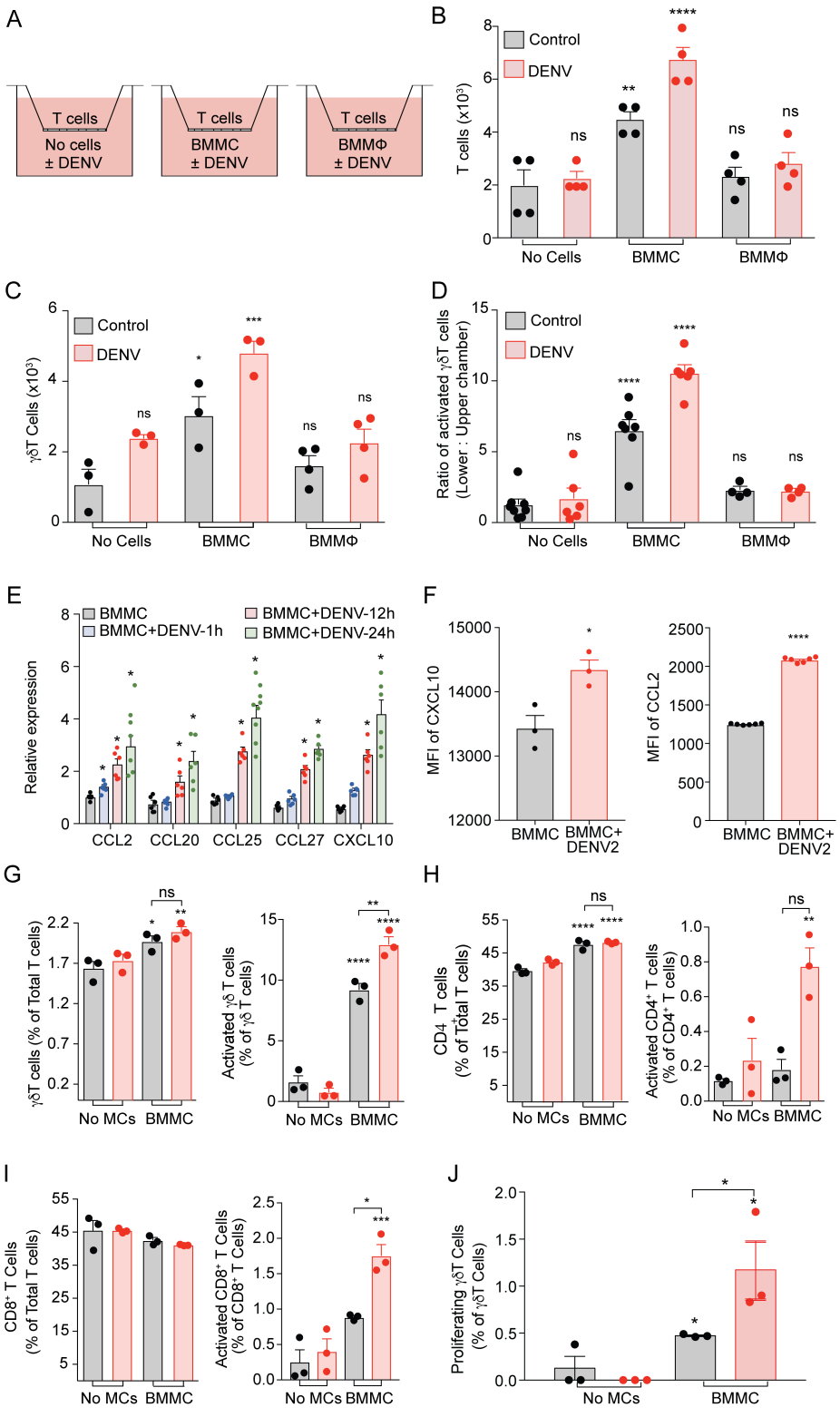

Figure 5: MC recruitment and contact-dependent activation and proliferation of γδ T cells. (**A**) Schematic showing the initial cell locations and conditions for the trans-well assay for panels **B-D**. BMMCs or BMMΦs were infected with DENV in the lower chamber and T cells (n=3

mice) were added to the top chamber to analyze migration and activation of T cell subsets across the trans-well (**B**) Significantly higher numbers of T cells migrated to the bottom chamber containing DENV2-stimulated MCs but not DENV2-infected BMMΦs. (**C**) Among the T cells that migrated to the lower chamber, the γδT cell subset was enriched in a MC-dependent manner. (**D**) Ratio of activated γδT cells ($CD3^+$γδTCR^+CD69^+) in the lower to upper chamber shows a significant increase in response to DENV2-stimulated MCs. (**E**) DENV2-stimulated expression of γδ T cell chemoattractants in MCs (**F**) Intracellular staining for chemokines showed increased CXCL10 and CCL2 production by DENV-treated MCs, 24h post challenge with DENV, measured by flow cytometry. (**G-I**) T cells isolated were cultured with BMMC in presence or absence of DENV to assess MC-dependent and DENV-dependent activation and proliferation. Cells were stained for CD3, CD4, CD8, CD69 and γδTCR and analyzed by flow cytometry after 96h of co-culture. The percentages of total and activated (**G**) γδ (**H**) $CD4^+$ and (**I**) $CD8^+$ T cells were compared. (**J**) T cells were labeled with CFSE prior to co-culture with BMMCs and the percentage of proliferating γδT cells was measured by flow cytometry. Representative flow cytometry plots are included as **Figure S11-12**. For all panels, Data represent mean±SEM; *p<0.05, **p<0.01, ***p<0.001, and ****p<0.0001. Statistical significance was assessed by two-way ANOVA with Tukey's post-test for panels **B-E**, by Student's unpaired t-test, 2-tailed for panel **F**, and by one-way ANOVA with Tukey's post-test for panels **G-J**. MCs induce antigen-dependent activation and proliferation of CD4, CD8 and γδT cells.

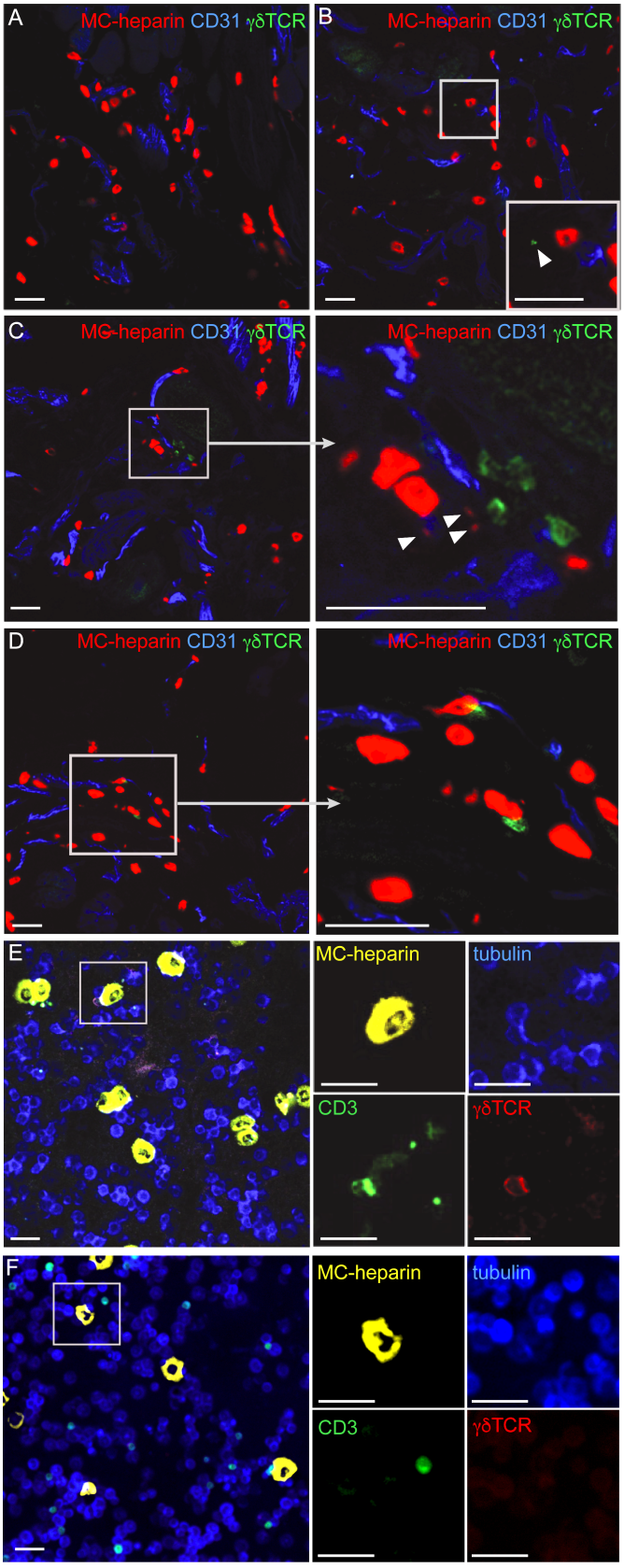

Figure 6: Immunological synapse formation between MCs and γδ T cells at infection sites. Mice (n=3) were injected with (**A-B**) saline or (**C-E**) 1×10^5 pfu of DENV. FP tissue collected 24h post-infection was sectioned and stained for blood vessels (CD31, blue), γδ TCR (green) and probed for MC-heparin (MC granules, red). Representative control confocal images are shown where MCs can be viewed near blood vessels (**A**) without nearby γδ T cells or (**B**) where γδ T cells appear infrequently in the same field as MCs. The area in the grey box is enlarged as an inset in **b**, and white arrowheads indicate γδ T cells. (**C**) In DENV-infected tissues, several γδ T cells cluster around MCs that appear activated due to MC granules that are extracellular in the tissue (indicated by white arrowheads in the enlarged inset on the right side). (**D**) Many γδ T cells were observed forming close contacts with MCs in DENV-infected tissues. Quantification of MC-γδ T cell contacts and additional representative images are provided in **Figure S13.** (**E**) MCs and γδ T cells were observed interacting in the peritoneal cavity 24h after i.p. infection with DENV (1×10^6 pfu). Peritoneal lavage cells were cytospun onto glass slides prior to staining with antibodies against CD3, γδ TCR, and tubulin and probing against MC-heparin. MCs and γδ T cells appeared to form stable contacts that were visualized after isolation. Strong polarization of CD3 and γδ TCR towards the MC contact site reveals immune synapse formation. (**F**) No stable contacts between MCs and γδ T cells were observed in cytospins from similarly prepared uninfected peritoneal cells. Additional representative images of MC-γδ T cell conjugates in cytospins of DENV-infected mice and of control cytospins are provided in **Figure S14**. Scale bars for all panels=20μm.

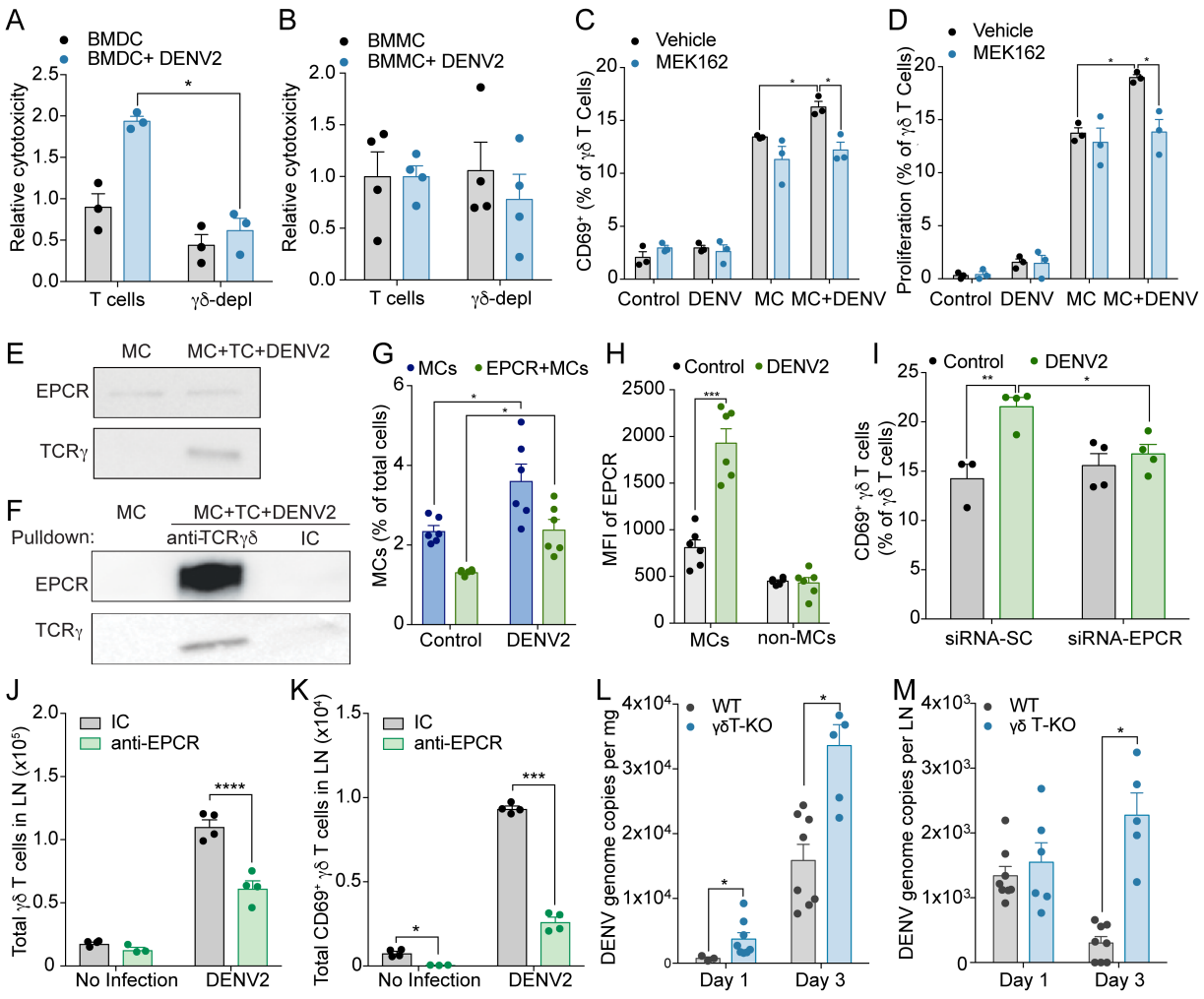

Figure 7: MC- and antigen-dependent γδT cell activation is mediated through EPCR and γδTCR, promoting viral clearance. Total T cells or T cells depleted of γδT cells, from DENV-infected LNs, 72h post-infection were co-cultured with (**A**) BMDCs or (**B**) BMMCs that were pre-infected with DENV (MOI-1). Cytotoxicity was measured by LDH assay and normalized to control. BMDCs but not BMMCs showed cytotoxicity, which was lost with γδT depletion. (**C-D**) CFSE-labeled T cells purified from naïve mice were co-cultured with BMMC±DENV and ±MEK162. MEK162 inhibited DENV-specific γδT cell (**C**) activation and (**D**) proliferation, measured by flow cytometry at 96h. (**E**) Lysates were from co-cultures of DENV-exposed MCs and T cells (TC) or control MCs were probed for EPCR by western blotting. γδTCR was only detected in lysates containing T cells (**F**) Pull-down of the γδTCR shows interaction with EPCR, detected by western blotting. Pulldown was confirmed by detection of the γTCR-subunit. In contrast, pull-down using an isotype control (IC) antibody did not precipitate γδTCR or EPCR. Increases in (**G**) MCs expressing EPCR and (**H**) expression of EPCR on MCs in LNs was observed at 24h post-infection. Representative flow cytometry plots are provided, **Figure S16**. (**I**) γδT cells are activated by DENV-exposed MCs transfected with scrambled-control siRNA, which was blocked by knock-down of EPCR in MCs. Blocking EPCR in vivo by injection of blocking antibody limits (**J**) accumulation and (**K**) activation of γδT cells in the draining LN following DENV infection. (**L-M**) WT and γδT-KO mice were infected with DENV2 by FP injection and DENV genome copies were quantified in the FPs and draining LNs at 24h and 72h

post-infection. γδT-KO mice had higher viral load in the (**L**) FP and (**M**) the draining LN. Data represent mean±SEM, *p<0.05, **p<0.01 ****p<0.0001 by two-way ANOVA (Sidak's multiple comparison test). N=4-6 per group.